# ANALYSIS OF WIND SPEED SHEAR AND TURBULENCE LIDAR MEASUREMENTS TO SUPPORT OFFSHORE WIND IN THE NORTHEAST UNITED STATES

**Dr. Anthony Viselli, PE**
University of Maine
Orono, Maine, U.S.A.

**Mr. Nathan Faessler**
University of Maine
Orono, Maine, U.S.A.

**Mr. Matthew Filippelli**
AWS Truepower
Albany, New York, U.S.A.

## ABSTRACT

This paper presents wind speed measurements collected at 40m to 200m above sea-level to support the New England Aqua Ventus I 12 MW Floating Offshore Wind Farm to be located 17km offshore the Northeast United States. The high-altitude wind speed data are unique and represent some of the first measurements made offshore in this part of the country which is actively being developed for offshore wind. Multiple LiDAR measurements were made using a DeepCLiDAR floating buoy and LiDARs located on land on a nearby island. The LiDARs compared favorably thereby confirming the LiDAR buoy measurements. Wind speed shear profiles are presented. The measurements are compared against industry standard mesoscale model outputs and offshore design codes including the American Bureau of Shipping, American Petroleum Institute, and DNV-GL guides. Significant variation in the vertical wind speed profile occurs throughout the year. This variation is not currently addressed in offshore wind design standards which typically recommend the use of only a few values for wind shear in operational and extreme conditions. The mean wind shears recorded were also higher than industry recommended values. Additionally, turbulence measurements made from the LiDAR, although not widely accepted in the scientific community, are presented and compared against industry guidelines.

## INTRODUCTION

There is an increased need to characterize the high altitude (greater than 40m above sea level) wind conditions offshore as offshore wind energy is developed to meet the increasing renewable energy demand in the Northeast US. Such measurement campaigns provide valuable data to support project design activities and provide unique measurements of the environmental conditions far offshore which have not been extensively measured at this time. This paper presents measurements of wind shear and turbulence measurements made by a floating light imaging, detection and ranging instrument (LiDAR) buoy, and a nearby land-based LiDAR, located 12 miles offshore the coast of Maine in the Northeast United States. Wind shear is caused primarily by the stability of the atmosphere which is governed by variation in the air temperature due to heating or cooling of the earth's surface. The location is adjacent to the proposed New England Aqua Ventus I Floating Offshore Wind Demonstration Project[1] (NEAV). This demonstration project consists of two 6 MW turbines on floating concrete semi-submersible hulls [1]. Each floating hull/turbine is held in position by three marine mooring lines anchored to the seabed, with the electrical generation connected by a subsea cable to the Maine power grid onshore. Once installed, the turbines will produce energy for 20-years.

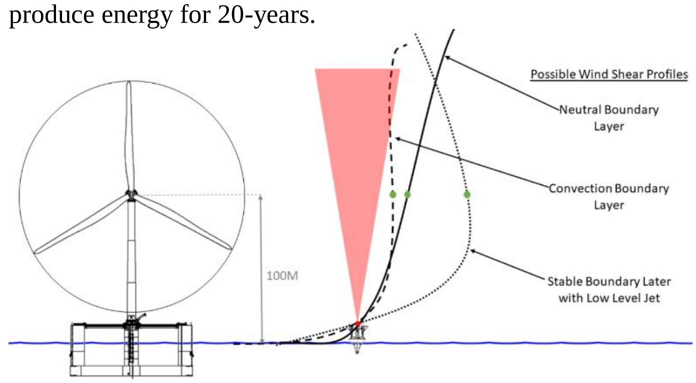


**Figure 1 Possible Wind Shear Profiles Offshore**

This paper summarizes wind shear and turbulence measurements made by the LiDAR devices and compares them with published design guides for offshore wind turbines. Wind shear is typically represented in the design codes with a power law model with a few wind shear exponents. However, it is well known that a variety of wind shear profiles are possible due to different boundary layer conditions as shown in Figure 1. There is currently little if any wind speed data offshore in the US at high altitudes needed to confirm the wind speed shear offshore

[1] http://maineaquaventus.com/

at this time as few projects have been built. Differences from diurnal and seasonal variance is investigated and presented. Wind turbulence measurements made by LiDAR, although not widely accepted as a valid measurement, are also presented as there are little if any offshore turbulence measurements currently in the public domain.

These early offshore measurements made in the North Atlantic and preliminary findings provide useful insights into the behavior of the wind speed profile far offshore in the Northeast US and will help, as more data becomes available from other projects, support increased understanding and aid improvement of design methods and standards.

## NOMENCLATURE

ABS: American Bureau of Shipping
API: American Petroleum Institute
ASCE: American Society of Civil Engineers
CNR: Carrier-to-Noise Ratio
DOE: US Department of Energy
DTU: Technical University of Denmark
Hub-height: Height of wind turbine rotor center above mean sea-level (m)
H: Reference height above sea-level
Hs: Significant Wave Height (m)
IEC: International Electrotechnical Commission
LiDAR: Light Imaging, Detection, and Ranging Instrument
MASS1: Mesoscale Atmospheric Simulation System
MSL: Mean Sea Level
NEAV: New England Aqua Ventus I Project
NED: National Elevation Database
NLCD: National Land Cover Dataset
NREL: National Renewable Energy Laboratory
STD: Standard Deviation
TI: Turbulence Intensity
USGS: US Geological Survey
α: Wind shear power law exponent
$H$: Height (m)
$u$: Wind speed (m/s)
$u'$: Root-mean-square of velocity fluctuation (Standard deviation)
$u_{avg}$: Average wind speed (m/s)
$u_{Xm}$: Wind speed (m/s) at a height X (m)
$z_r$: Reference height (m)
$z$: Height (m)
$z_o$: Logarithmic wind shear law roughness parameter (m)

## PAST OFFSHORE MEASUREMENTS AND APPROXIMATIONS FOR WIND SHEAR/ TURBULENCE

Although there is a wealth of near surface data collected from oceanographic buoys, at this time there are few public data sets for offshore wind speed measurements at wind turbine hub heights (~100 m) available in the US. A brief summary of known offshore public data sets and assumed wind shear and turbulence parameters is presented to provide context to the new measurements made in this study. The US Department of Energy (DOE) launched a Wind Sentinel LiDAR buoy off the coast of Virginia in 2016. The buoy collected mean wind profiles which consistently showed wind speed maxima at about the 90 m level as well as negative shears above 90m. The maximum in the wind speed profile at 90m was thought to be due to the slow biases in the upper range gates from the influence of systematic noise when the backscatter signal is weak [2]. Additionally, the DOE launched a similar campaign in Atlantic City, New Jersey.

The National Renewable Energy Laboratory (NREL) has published US offshore wind resource maps which present mean annual wind speeds at turbine hub heights of 90m. These plots have assumed an average wind shear exponent of 0.11 [3]. Please see equation 1 for the wind shear power law in the subsequent section. This was further shown to be accurate when compared to California data where similar 90m wind speeds were calculated using this exponent between 50m to 70m. Similar studies of the great lakes have used shear coefficients of 0.10 in Lake Erie and Lake Ontario [4]. The University of Maine, with the use of metocean buoy data including surface level wind speed data and published mean wind speeds from NREL, estimated wind shear coefficients [5]. A short one-month campaign of ship mounted LiDAR measurements was performed off the coast of Maine in the summer of 2004 and showed a range of wind shear values between -0.02 and 0.06 [6].

In Europe more data for wind shear exists likely due to the number of offshore wind farms currently installed. However, much of this data is proprietary and not in the public domain. It has been shown that with traditional methods, such as the Monin-Obukhox profile, wind shear in the surface layer is often under estimated. It was observed that wind shear is often larger than predictions from traditional methods, especially in warmer air conditions [7]. This suggests that traditional methods may need to be modified where atmospheric stability is accounted for. Furthermore, the Technical University of Denmark (DTU) has performed studies in the North Sea using LiDAR devices. From this they have concluded that "current wind engineering commonly-used wind shear norms and standards seem to be far too optimistic and not very conservative" [8]. The values from standards were generally lower than measurements. Studies performed by the DTU comparing wind shear measurements between met-masts and wind LiDARs in the North Sea show that the typically assigned offshore wind shear value of α=0.2, is only accurate for a very slim set of atmospheric and marine conditions [9]. Rather, it has been observed that wind shear values at 100m have a range between -0.2 to 0.8.

Public wind turbulence measurements offshore at hub-height appear to be scarce. Europe has more data for wind turbulence, but most of this data is still proprietary. Two years of analyzed data is available from a costal measurement station in Norway. This analysis shows that offshore and costal environments tend to have a turbulence intensity (TI) slightly less than the onshore sector. Furthermore, there is a distinct difference shown between seasons where the difference between these sectors is more pronounced in summer [10]. Multiple methods of predicting TI have been compared to measurements taken at the Greater Gabbard Offshore Wind Farm. This data set shows mean TI values between 0.07-0.10 between 3-25m/s wind speeds when taking into account all wind directions [11]. Both studies detail a difference between onshore and offshore sectors, however findings from the Greater Gabbard Offshore Wind Farm suggests this difference may be more pronounced than just a slight difference.

## SUMMARY OF OFFSHORE WIND ENERGY DESIGN STANDARDS REQUIREMENTS FOR WIND SHEAR AND TURBULENCE

Wind shear recommended design values are provided in offshore wind engineering design guides including the American Bureau of Shipping (ABS) Guide for Building and Classing Floating Offshore Wind Turbine Installations [12], the International Electrotechnical Commission (IEC) International Standard IEC 61400-3 [13], DNV-RP-C205 Environmental Conditions and Environmental Loads [14], and ASCE [15]. Table 1 presents a summary of the recommended wind shear values from these standards. The table shows that there is a significant difference between the standards. For example, the ABS guide differentiates between operational and extreme conditions while the other standards provide one value. The differences between the standards are significant. Consider that a 5m/s wind speed at 4m above sea-level, when sheared up to 100m hub height yields a wide range of wind speeds of 7.1, 9.5, 7.4, and 8.1m/s for the four standards listed in the order presented in Table 1.

**Table 1 Comparison of Offshore Wind Shear Design Values**

| Reference | ABS (operation/ extreme) [12] | IEC 61400-3 [13] | DNV-RP-C205 [14] | ASCE [15] |
|---|---|---|---|---|
| Wind Shear Exponent normal conditions | 0.11/0.14 | 0.20 | 0.12 | 0.15 |

Wind turbulence recommended design values and wind field models are given by IEC 61400-1 [16] for turbulence. ABS references this same set of turbulence requirements. The IEC models are based on 90% quantile turbulence measurement and provide turbulence intensity as a function of wind speed for the purposes of load calculation and to provide conservative estimates for fatigue damage accumulation. Additional details on the turbulence intensity models are presented with comparisons later in this paper.

## LIDAR MEASUREMENT PROGRAM

From 2014 to 2016, land-based and buoy mounted LiDAR wind measurements were collected on and near Monhegan Island. The island itself is roughly 17km form the mainland. Figure 2 shows a map of the two locations. The instruments and data collected can be found summarized in Table 2.

The measurements made consisted of both a land-based LiDAR unit, as well as a DeepCLiDAR Buoy in an open ocean environment just south of Monhegan Island. Both LiDARs were a Windcube type LiDAR produced by Leosphere. The offshore measurements were collected using a Windcube V2 Offshore LiDAR, while the land-based data are comprised of measurements from both a Windcube V2 Offshore LiDAR and a Windcube V1 LiDAR deployed at different times. The V2 LiDAR is the next iteration of the V1 LiDAR and there are no significant difference in the data between the units after completing side-by- side comparisons. The V2 Offshore LiDAR includes built in motion correction software to compensate for motions experienced by the buoy while at sea. Both LiDARs delivered data based on 10-minute averaging period. The data include mean wind speeds, wind speed variance, signal to noise ratio to assess quality, and direction at nine programmable levels from 40m-200m above the system.

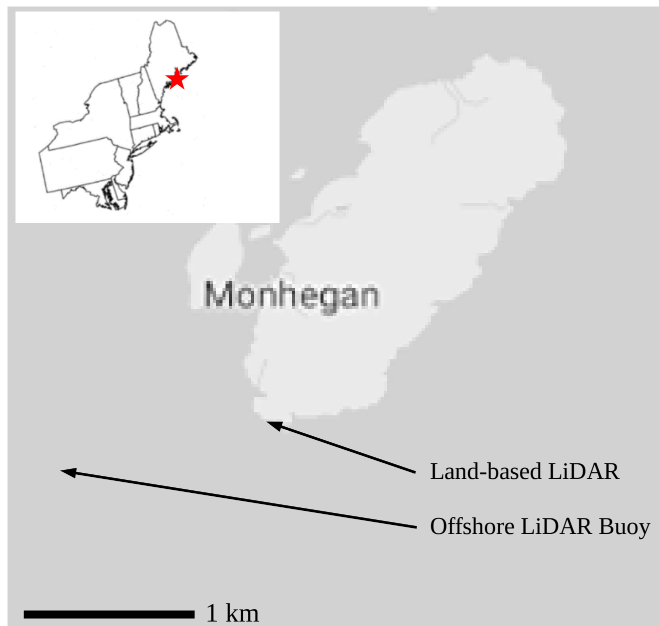


**Figure 2 LiDAR Deployment Test Sites**

In addition to providing hub-height offshore wind speed measurements, the effort allowed for the validation of the DeepCLiDAR buoy technology following the Carbon Trust Roadmap for floating LiDAR technologies [17] [18]. The effort showed that the LiDAR buoy meets the acceptance criteria of the carbon trust, which focused on a 6-month segment of the DeepCLiDAR launch. This analysis showed that the buoy data met the availability standards and wind speed/direction correlation standards. Figure 3 shows the setup of a land-based measurement site, positioned at the Southern tip of the island, roughly 1.2km east from the deployment site of the DeepCLiDAR Buoy offshore. The Windcube was positioned with a line-of-site to the LiDAR buoy with little obstruction. The land-based unit was powered via an extension cord connected to the island's power grid. An uninterruptable power supply was put in-line to deal with unreliable power issues that are common on Monhegan which has its own diesel-powered grid. The site provided a clear and open area for the LiDAR to take measurements.

Additionally, surface level wind speed and wave data from an existing nearby UMaine buoy, E01, was also collected during this time [19]. This served as another reference point for the measurements and was used to provide concurrent wave height data for the land-based LiDAR data discussed later.

**Table 2 Summary of Data Collected and Used in this Study**

| Station | Sensor Type | Elevation above MSL | Lat. & Lon. (DD MM) | Date Range | Average Sampling Period |
|---|---|---|---|---|---|
| Offshore, UMaine DeepCLiDAR Buoy | Wave | Surface | 43° 45´ 22.8"N<br>69° 20´ 21.0"W | 2/19/2016-10/28/2016 | 30-min |
| | Wind Speed LiDAR | 40-200m | | | 10-min |
| Land-based, Monhegan Island | Wind Speed LiDAR | 40-200m | 43° 45' 29.7" N<br>69° 19' 19.1" W | 3/18/2014-7/21/2014 | 10-min |
| | | | | 11/26/15-04/19/2017 | |
| Offshore, Reference Buoy E01 | Wave | Surface | 43° 42' 53.4"N<br>69° 21' 18.0"W | 7/9/2001-Present | 30-min |

Figure 4 shows the DeepCLiDAR deployed offshore near Lobster Cove. The water depth was roughly 95m and is approximately 1.26 km from Monhegan Island. Due to the distance between Monhegan Island and Maine's coastline, the site offered an open-ocean environment generally upwind of the island. The buoy collected 30-minute significant wave height and peak period measurements and 1 minute current speeds and directional data offshore which were used to assess the performance of the LiDAR wind speed measurements under these conditions. The buoy collected data for approximately seven months. A summary of sea state conditions at the buoy site is presented in Table 3.

**Figure 3 View of Land Based LiDAR from North/Northeast Looking South/Southwest over Lobster Cove, Monhegan Island**

**Table 3 Campaign Average and Maximum 1 Hour Significant and Maximum Wave Heights**

| Measurement | Average (m) | Maximum (m) | Average Wave Peak Period (s) |
|---|---|---|---|
| Significant Wave Height | 1.04 | 5.30 | 9.5 |
| Max Wave Height | 1.73 | 8.94 | |

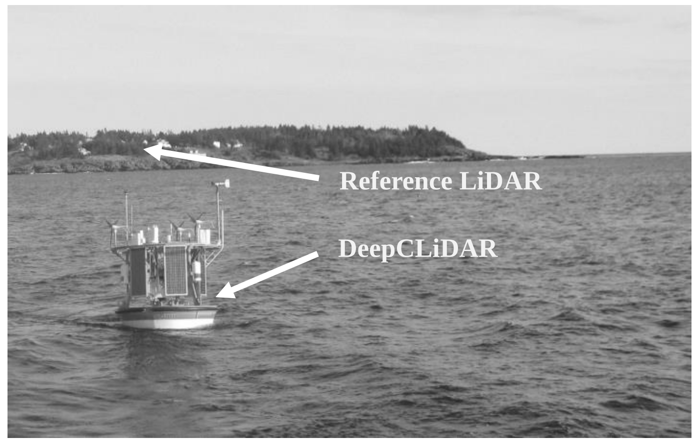


**Figure 4 View Looking North of the DeepCLiDAR Buoy System**

Table 4 summaries the basic wind measurements made by the land-based LiDAR and DeepCLiDAR. The mean and standard deviation of the 10-minute wind speed measurements is presented for each LiDAR using all data screened based on "data availability" for each 10-minute record. Data availability is determined by the carrier-to-noise ratio (CNR) and helps flag low signal strength which can lead to inaccurate measurements. This is a standard practice among LiDAR measurements in the wind industry and helps lead to higher quality data collection and analysis. Because the land-based measurement record is longer than the DeepCLiDAR measurement record, concurrent land-based LiDAR measurements are also provided to facilitate comparison of the two data sets. These values are displayed in parenthesis below the full data values.

**Table 4 Summary of Wind Speed Measurements taken by LiDAR Systems on Land and Offshore (Contemporaneous data is provided in parentheses for the Land-based measurements.)**

| Measurement | Land-based LiDAR | | Offshore DeepCLiDAR | |
|---|---|---|---|---|
| | Mean (m/s) | Std (m/s) | Mean (m/s) | Std (m/s) |
| 40m Wind Speed: All Data | 7.73 (7.28) | 3.62 (3.68) | 7.64 | 3.86 |
| 40m Wind Speed: Availability >90% | 7.58 (7.35) | 3.65 (3.63) | 7.68 | 3.85 |
| 100m Wind Speed: All Data | 8.96 (9.11) | 4.40 (4.78) | 9.21 | 4.62 |
| 100m Wind Speed: Availability >90% | 9.00 (9.24) | 4.52 (4.76) | 9.35 | 4.82 |

It is noted that the two LiDAR data sets have a difference in the mean and standard deviation. The mean and standard deviation values for the land-based and offshore LiDAR systems differ due to differences in geography, topography, and primarily the length and duration of the data record. The land-based LiDAR is significantly longer. This is expected and is important to consider when comparing the two data sets.

## WIND SHEAR DATA ANALYSIS

The method of calculating wind shear using a power law approach [20] is now presented. The wind profile power law was used to calculate a wind shear exponent value (α) by the solving the following formula for α:

$$(1)\ u = u_r\left(\frac{z}{z_r}\right)^{\alpha},$$

Where the variables are as defined in the nomenclature section. Two measurement heights ($z$) were selected to determine α. Wind speed measurements ($u$), in meters per second, taken at 40 and 100 meters were used. 100 meters was chosen because it represents the hub height for the proposed 6MW turbines. 40 meters was chosen because it offered the most available data out of the remaining measurement heights. This resulted in the power law being treated as such:

$$(2)\ u_{100m} = u_{40m}\left(\frac{100}{40}\right)^{\alpha}$$

Table 5, Table 6, and Table 7 show the measured wind shear values broken down into 2m/s bins for the all land-based measurements, concurrent land-based measurements, and the offshore buoy measurements respectively. Table 6 presents only the contemporaneous data measured by the Land-based LiDAR for the purposed of comparing with the offshore LiDAR measurements. Statistical data is provided for each bin. Both of the two LiDAR measurement campaigns generated over 24,000 10-minute wind speed samples (over 167 days). The final row includes data below 1m/s and above 27m/s and therefore an additional 221 and 271 data points are included. As expected based on the annual wind speed distribution, not all of the wind speed bins have an equal amount of data. For both the land-based and DeepCLiDAR measurements, about 90% of the data occurs when the average wind speed is below 17m/s.

The data show a wide range of mean-wind shear values for the different wind-speed bins and significant variation within each bin as indicated by the standard deviation and $10^{th}$/ $90^{th}$ percentile values. The lower wind-speed bins have low wind shear exponents and generally increases with the average 10-minute wind speed bin. For the lowest wind speed bin of 1-3m/s, the wind shear exponent is highly variable and the mean is negative. However, these speeds are typically not studied since the cut in speed for most turbines is 4m/s. The average wind shear exponent for wind speed bins above 11m/s fall above 0.26 and 0.21 for the land-based and DeepCLiDAR data sets respectively. These values are above the recommended industry standards in Table 1. The overall average wind shear exponent using the contemporaneous data for the land-based and DeepCLiDAR buoy are 0.23 and 0.15.

**Table 5 Land-based Reference LiDAR Measured Wind Shear Exponent, α. (All data is considered.)**

| Wind Speed Bins (m/s) | Mean | Standard Deviation | $10^{th}$ Percentile | 90th Percentile | Number of Data Points |
|---|---|---|---|---|---|
| **1-3** | -0.05 | 0.52 | -0.70 | 0.57 | 1,722 |
| **3-5** | 0.12 | 0.33 | -0.24 | 0.51 | 2,814 |
| **5-7** | 0.19 | 0.22 | -0.04 | 0.48 | 3,875 |
| **7-9** | 0.23 | 0.20 | 0.02 | 0.50 | 3,909 |
| **9-11** | 0.25 | 0.18 | 0.03 | 0.49 | 3,519 |
| **11-13** | 0.26 | 0.18 | 0.04 | 0.47 | 2,776 |
| **13-15** | 0.24 | 0.15 | 0.04 | 0.42 | 2,153 |
| **15-17** | 0.25 | 0.13 | 0.05 | 0.41 | 1,716 |
| **17-19** | 0.27 | 0.12 | 0.08 | 0.41 | 913 |
| **19-21** | 0.28 | 0.11 | 0.13 | 0.39 | 210 |
| **21-23** | 0.30 | 0.10 | 0.19 | 0.46 | 251 |
| **23-25** | 0.27 | 0.09 | 0.17 | 0.35 | 136 |
| **25-27** | 0.20 | 0.04 | 0.15 | 0.24 | 66 |
| **All Data** | 0.20 | 0.28 | -0.03 | 0.24 | 24,281 |

**Table 6 Land-based Reference LiDAR Measured Wind Shear Exponent, α. (Only concurrent measurements with offshore LiDAR are considered.)**

| Wind Speed Bins (m/s) | Mean | Standard Deviation | $10^{th}$ Percentile | 90th Percentile | Number of Data Points |
|---|---|---|---|---|---|
| **1-3** | -0.09 | 0.57 | -0.76 | 0.63 | 1284 |
| **3-5** | 0.14 | 0.38 | -0.29 | 0.59 | 2023 |
| **5-7** | 0.22 | 0.25 | -0.08 | 0.53 | 2702 |
| **7-9** | 0.27 | 0.20 | 0.03 | 0.52 | 2837 |
| **9-11** | 0.30 | 0.18 | 0.09 | 0.53 | 2585 |
| **11-13** | 0.30 | 0.17 | 0.10 | 0.51 | 2048 |
| **13-15** | 0.28 | 0.16 | 0.06 | 0.46 | 1434 |
| **15-17** | 0.29 | 0.13 | 0.07 | 0.44 | 1126 |
| **17-19** | 0.31 | 0.10 | 0.15 | 0.42 | 631 |
| **19-21** | 0.30 | 0.10 | 0.15 | 0.41 | 153 |
| **21-23** | 0.32 | 0.10 | 0.21 | 0.47 | 189 |
| **23-25** | 0.29 | 0.09 | 0.19 | 0.43 | 97 |
| **25-27** | 0.20 | 0.04 | 0.15 | 0.26 | 32 |
| **All Data** | 0.23 | 0.31 | -0.08 | 0.51 | 17306 |

**Table 7 DeepCLiDAR Measured Wind Shear Exponent, α**

| Wind Speed Bins (m/s) | Mean | Standard Deviation | 10th Percentile | 90th Percentile | Number of Data Points |
|---|---|---|---|---|---|
| **1-3** | -0.07 | 0.48 | -0.66 | 0.58 | 2,120 |
| **3-5** | 0.10 | 0.35 | -0.26 | 0.53 | 3,429 |
| **5-7** | 0.15 | 0.24 | -0.08 | 0.47 | 4,521 |
| **7-9** | 0.17 | 0.20 | -0.03 | 0.43 | 5,036 |
| **9-11** | 0.20 | 0.18 | 0.01 | 0.43 | 4,450 |
| **11-13** | 0.21 | 0.16 | 0.03 | 0.41 | 3,460 |
| **13-15** | 0.21 | 0.14 | 0.03 | 0.38 | 2,167 |
| **15-17** | 0.24 | 0.12 | 0.04 | 0.38 | 1,700 |
| **17-19** | 0.26 | 0.11 | 0.07 | 0.38 | 882 |
| **19-21** | 0.27 | 0.09 | 0.16 | 0.36 | 287 |
| **21-23** | 0.29 | 0.09 | 0.16 | 0.44 | 207 |
| **23-25** | 0.25 | 0.08 | 0.15 | 0.33 | 91 |
| **25-27** | 0.21 | 0.05 | 0.13 | 0.25 | 7 |
| **All Data** | 0.15 | 0.27 | -0.09 | 0.42 | 28,628 |

Figure 5, Figure 6, and Figure 7 present a scatter diagram of the measured wind shear exponents for the Land-based and buoy LiDAR measurements versus 10-minute mean wind speed at 100m above Mean Sea-Level. The mean wind shear exponent for each 2m/s bin and the 10$^{th}$ and 90$^{th}$ percentile for each bin are also plotted. The data shows a slow and steady climb in wind shear coefficient as wind speed increases, up until roughly 24m/s, however, it is unclear whether this drop is due to a physical phenomenon or due to a lack of data measurements at these higher wind speeds.

## ESTIMATES OF WIND SHEAR USING A MESOSCALE MODEL

Estimates of wind shear exponents at the site were also made using a mesoscale model and are presented in Table 8. The model was used to predict the monthly average wind shear coefficient. The model estimates the wind shear for each hour of the day for each month. The values reported here are the average of the hourly average wind shear coefficients predicted by the model for each day. The data shows a difference in mean wind shear throughout the year ranging from 0.05 to 0.19. Summer months exhibit the highest wind shear while winter typically experiences lower wind shear values. The mesoscale model used is the Mesoscale Atmospheric Simulation System (MASS1), which was run in a series of nested grids, with the innermost grid having a spatial resolution of 1.2 km. The microscale model (WindMap) further refined this output to a horizontal grid spacing of 50 m. The source of topographic data was the National Elevation Dataset (NED), a digital terrain model produced on a 30 m grid by the US Geological Survey (USGS). The source of land cover data was the 30 m resolution National Land Cover Dataset (NLCD), which is produced by the USGS and derived from Landsat imagery. While the majority of the mapped study area is open water, the land cover and topographic data was necessary to properly characterize wind flows over land features like Monhegan Island. In converting from land cover to surface roughness, the onshore roughness length values that were applied are believed to be typical of conditions in coastal Maine. However, the roughness could vary a good deal within each onshore class, potentially affecting the wind in the near shore environments.

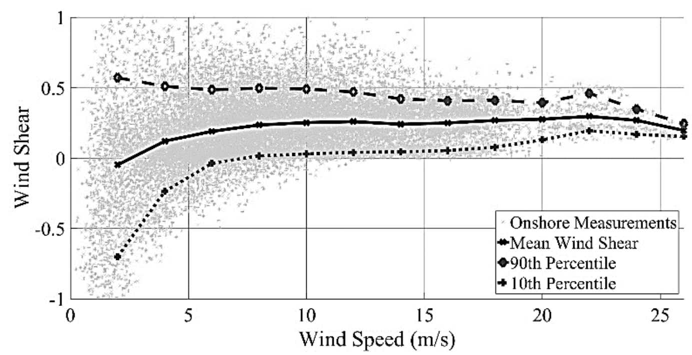


**Figure 5 Reference LiDAR Measured Wind Shear v. 100m Wind Speed Data for All Data**

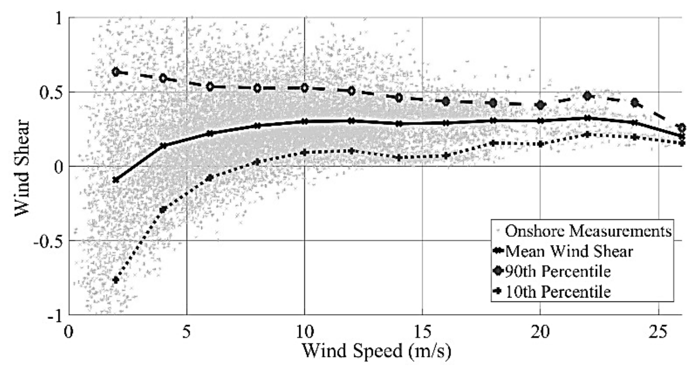


**Figure 6 Reference LiDAR Measured Wind Shear v. 100m Wind Speed Data for Contemporaneous Data Only**

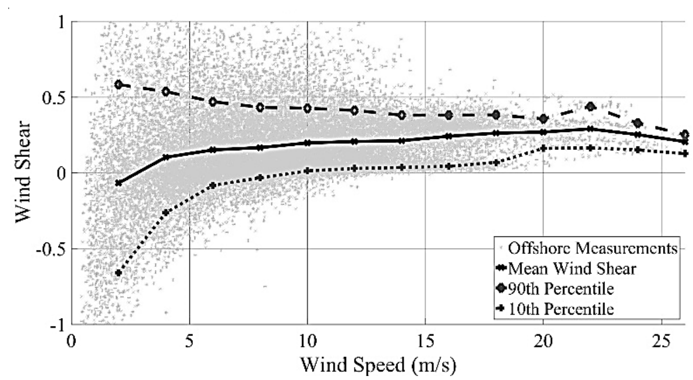


**Figure 7 DeepCLiDAR Measured Wind Shear v 100m Wind Speed With Data**

The predictions of the model are compared to the measured average 10-minute wind shear measured by the land-based and offshore LiDARs. In general the measured wind shear is noticeably higher than the model predictions.

**Table 8 Mesoscale Model Predicted Wind Shear Exponents**

| | Average Wind Shear Coefficient, α | | |
|---|---|---|---|
| **Month** | **Mesoscale Model** | **Reference LiDAR Measurements** | **DeepCLiDAR Measurements α** |
| Jan | 0.05 | 0.12 | NA |
| Feb | 0.06 | 0.16 | 0.13 |
| Mar | 0.10 | 0.22 | 0.09 |
| Apr | 0.14 | 0.24 | 0.13 |
| May | 0.17 | 0.26 | 0.15 |
| Jun | 0.18 | 0.22 | 0.18 |
| Jul | 0.19 | 0.23 | 0.19 |
| Aug | 0.18 | 0.25 | 0.22 |
| Sep | 0.16 | 0.08 | 0.13 |
| Oct | 0.11 | 0.24 | 0.13 |
| Nov | 0.08 | 0.17 | NA |
| Dec | 0.06 | 0.12 | NA |
| **Yearly Average** | **0.12** | **0.20** | **0.15** |

## WIND TURBULENCE INTENSITY MEASURMENTS

Industry confidence in turbulence intensity values calculated using LiDAR measurements is not fully accepted. Turbulence characteristics of atmospheric flows can be derived from LiDAR measurements, but it is not nearly as established other methods **[21]**. When using vertical profilers, such as LiDAR, turbulence measurements generally experience two sources of error. Variance is reduced due to the volumetric averaging of radial velocity measurements. Furthermore, variance is also effected by the cross contamination due to the scanning geometry of the LiDAR **[22]**. Issues with variance from a WindCube LiDAR specifically have been observed in a comparison of multi-LiDAR methods of measuring turbulence. Unstable conditions further showed variance contamination in horizontal measurements from the WindCube when compared to the multi-LiDAR setups **[23]**. Other researchers have developed more sophisticated methods of using multiple LiDARs to obtain more reliable wind turbulence measurements **[23]**. Although the use of LiDAR for turbulence has known limitations, the data collected here is useful given that little if any turbulence data offshore the northeast US exists in the public domain. In this study, the turbulence intensity was calculated directly from the LiDAR which is equal to the standard deviation divided by the mean of a 10-minute wind speed record. Table 9, Table 10, and Table 11 present the turbulence intensity data made from the Land-based and DeepCLiDAR wind speed measurements at 100m. The TI can be found with the collected data with the use of standard deviation of the wind velocity ($\boldsymbol{u'}$) over the mean wind velocity ($\boldsymbol{u_{avg}}$) **[14]**:

$$(3)\ TI = \frac{u'}{u_{avg}}$$

**Table 9 Land-based Reference LiDAR Wind Turbulence Intensity at 100m Using All Data**

| Wind Speed Bins (m/s) | Mean | Standard Deviation | 10th Percentile | 90th Percentile | Number of Data Points |
|---|---|---|---|---|---|
| **1-3** | 0.265 | 0.136 | 0.111 | 0.455 | 1722 |
| **3-5** | 0.139 | 0.067 | 0.057 | 0.225 | 2815 |
| **5-7** | 0.098 | 0.043 | 0.044 | 0.154 | 3878 |
| **7-9** | 0.077 | 0.036 | 0.033 | 0.126 | 3909 |
| **9-11** | 0.063 | 0.032 | 0.023 | 0.103 | 3519 |
| **11-13** | 0.056 | 0.027 | 0.021 | 0.090 | 2776 |
| **13-15** | 0.055 | 0.026 | 0.020 | 0.087 | 2153 |
| **15-17** | 0.045 | 0.021 | 0.017 | 0.074 | 1716 |
| **17-19** | 0.037 | 0.019 | 0.014 | 0.063 | 913 |
| **19-21** | 0.042 | 0.013 | 0.025 | 0.058 | 210 |
| **21-23** | 0.041 | 0.011 | 0.029 | 0.053 | 251 |
| **23-25** | 0.041 | 0.010 | 0.030 | 0.053 | 136 |
| **25-27** | 0.047 | 0.007 | 0.041 | 0.054 | 66 |
| **All Data** | 0.093 | 0.085 | 0.026 | 0.174 | 24285 |

**Table 10 Land-based Reference LiDAR Wind Turbulence Intensity at 100m Using Contemporaneous Data**

| Wind Speed Bins (m/s) | Mean | Standard Deviation | 10th Percentile | 90th Percentile | Number of Data Points |
|---|---|---|---|---|---|
| **1-3** | 0.235 | 0.129 | 0.098 | 0.422 | 1284 |
| **3-5** | 0.117 | 0.062 | 0.050 | 0.191 | 2024 |
| **5-7** | 0.082 | 0.039 | 0.039 | 0.131 | 2705 |
| **7-9** | 0.064 | 0.032 | 0.029 | 0.106 | 2837 |
| **9-11** | 0.052 | 0.029 | 0.021 | 0.087 | 2585 |
| **11-13** | 0.048 | 0.025 | 0.018 | 0.081 | 2048 |
| **13-15** | 0.045 | 0.025 | 0.018 | 0.076 | 1434 |
| **15-17** | 0.037 | 0.021 | 0.015 | 0.067 | 1126 |
| **17-19** | 0.030 | 0.017 | 0.013 | 0.056 | 631 |
| **19-21** | 0.039 | 0.013 | 0.016 | 0.058 | 153 |
| **21-23** | 0.039 | 0.011 | 0.029 | 0.050 | 189 |
| **23-25** | 0.039 | 0.009 | 0.030 | 0.048 | 97 |
| **25-27** | 0.045 | 0.005 | 0.038 | 0.052 | 32 |
| **All Data** | 0.080 | 0.078 | 0.022 | 0.090 | 17310 |

**Table 11 DeepCLiDAR Measured Wind Turbulence Intensity at 100m**

| Wind Speed Bins (m/s) | Mean | Standard Deviation | 10th Percentile | 90th Percentile | Number of Data Points |
|---|---|---|---|---|---|
| **1-3** | 0.252 | 0.111 | 0.228 | 0.408 | 2127 |
| **3-5** | 0.138 | 0.063 | 0.124 | 0.209 | 3434 |
| **5-7** | 0.103 | 0.042 | 0.095 | 0.157 | 4523 |
| **7-9** | 0.091 | 0.037 | 0.085 | 0.142 | 5036 |
| **9-11** | 0.083 | 0.036 | 0.076 | 0.131 | 4450 |
| **11-13** | 0.081 | 0.032 | 0.076 | 0.126 | 3460 |
| **13-15** | 0.083 | 0.030 | 0.079 | 0.123 | 2167 |
| **15-17** | 0.082 | 0.028 | 0.077 | 0.121 | 1700 |
| **17-19** | 0.080 | 0.026 | 0.079 | 0.117 | 882 |
| **19-21** | 0.094 | 0.021 | 0.090 | 0.118 | 287 |
| **21-23** | 0.091 | 0.015 | 0.089 | 0.113 | 207 |
| **23-25** | 0.091 | 0.014 | 0.090 | 0.108 | 91 |
| **25-27** | 0.095 | 0.007 | 0.091 | 0.103 | 7 |
| **All Data** | 0.110 | 0.075 | 0.050 | 0.176 | 28642 |

When considering the concurrent data, the onshore LiDAR generally showed smaller turbulence intensity for all wind speeds. This is possibly due to the motion of the buoy, although there is motion correction applied to the measurements by the manufacturer. Additionally, the difference could also be due to the geographical location and topography of the two sites.

## DISCUSSION: COMAPRISON OF DATA WITH INDUSTRY DESIGN GUIDES

A comparison of the measured wind shear exponents against industry recommended design values is now presented. Table 12 presents a comparison of the measured exponents from the two LiDARs against DNV, ABS, ASCE, API, the mesoscale model estimates, and a previous study based on published buoy wind speed data at sea-level and published hub-height values [5]. The exponents from DNV-RP-C205 were calculated by converting from a surface roughness value to a wind shear exponent value using equation 2.3.2.9 [14]:

$$(4)\quad \alpha = \frac{\ln\left(\frac{\frac{z}{z_0}}{\frac{H}{z_0}}\right)}{\ln\left(\frac{z}{H}\right)}$$

This equation is a combination of logarithmic and power law wind profiles and is height dependent. Here H is equal to 40 meters and z is equal to 100 meters to be consistent with wind shear value calculation process.

The API estimates for power law exponent and log profile roughness parameter were calculated following equations A.2, A.3, and A.4 from standard APR RP 2MET [24] for a one hour wind speed of 20 m/s, and converted to a ten-minute mean wind speed. The API logarithmic wind shear model is different from the DNV model. Offshore Maine, the one year mean wind speed at 4m above sea level is equal to 21.4m/s at the location of this experiment which, when converted to 1-hour averaging period, is equivalent to 20m/s [5]. This wind speed was used for the purposes of comparison of the values estimated here. An equivalent roughness coefficient and wind shear exponent were calculated between 40m and 100m elevations for the purposes of comparing with the other standards. The API model is representative of offshore conditions, in strong, nearly neutrally stable atmospheric wind conditions during storms.

**Table 12 Coastal wave environment and its relation to wind shear coefficient and roughness parameter**

| Source | Terrain Type | α | $Z_0$ |
|---|---|---|---|
| **Land-based LiDAR** | Coastal area with small waves (<1m) | 0.20 | 0.190 |
| | Coastal area with medium waves (1<Hs<3m) | 0.19 | 0.144 |
| | Coastal area with large waves (Hs>3m) | 0.20 | 0.190 |
| | All data | 0.20 | 0.190 |
| **Offshore DeepCLiDAR Buoy** | Open sea with small waves (<1m) | 0.14 | 0.023 |
| | Open sea with medium waves (1<Hs<3m) | 0.18 | 0.108 |
| | Open sea with large waves (Hs>3m) | 0.19 | 0.144 |
| | All data | 0.15 | 0.035 |
| **DNV RP-C205** [14] | Offshore without waves | 0.07 | 0.0001 |
| | Offshore with large waves | 0.07 | 0.010 |
| | Coastal areas with onshore wind (low value) | 0.11 | 0.001 |
| | Coastal areas with onshore wind (high value) | 0.09 | 0.010 |
| **ABS** [12] | Offshore- Normal winds | 0.14 | 0.036 |
| | Offshore- Extreme winds | 0.11 | 0.003 |
| **API RP 2MET** [24] | 20m/s wind speed at 10m above sea level | 0.08 | 0.0004 |
| **IEC 61400-3** [13] | Offshore- Normal winds | 0.20 | 0.190 |
| | Offshore- Extreme winds | 0.20 | 0.190 |
| **ASCE-7** [15] | Offshore- annual average | 0.16 | 0.054 |
| **Viselli et al** [5] | Offshore- annual average | 0.12 | 0.120 |
| **Mesoscale Model** | Annual average | 0.12 | 0.009 |

Several wind shear parameters are presented for each data set and industry standard when available based on the roughness of the sea surface which is characterized by the significant wave height conditions. The DeepCLiDAR buoy provides both wind and wave measurement instrumentation which allows for the data to be screened and a separate mean wind shear to be reported for different significant wave height, Hs, ranges. In this study low waves were considered below 1m. Medium Hs was considered to be greater than 1m and less than 3m. Large waves were considered greater than 3m. The majority of the waves were below 1m. 62% of data had a wave height less than 1m, 36% was between 1m to 3m, and only 2% of data is for wave heights greater than 3m.

The land-based LiDAR was similarly treated except concurrent significant wave height data was taken from the other nearby reference buoy, E01. E01 is roughly 5.5km southwest from the land-based collection site. The majority of waves at E01 fall under 3m. 46% of the data had a Hs less than 1m, 50% with a Hs between 1m to 3m, and 4% with an Hs greater than 3m. These alternate wind shear values are presented and allow for comparison against industry standards which provide typical wind shear values for different sea conditions.

DNV RP-C205 presents a wide range of wind shear values for offshore and coastal conditions based on the wave conditions. The other standards do not present explicit wind shear conditions based on wave heights. ABS and IEC present a normal and extreme wind shear only. The normal wind shear is likely more typical of a low to medium wave environment and the extreme wind shear could be considered more close to the larger wave environmental conditions.

The offshore LiDAR average shear exponent of 0.15 exceeds the offshore DNV range of 0.08 to 0.13, the ABS values of 0.11 to 0.14, the previous study by Viselli et al and the Mesoscale model prediction. This data is less than the 0.2 value recommended by IEC 61400-3 and the 0.16 value proposed by ASCE-7. As compared to API, the measured wind shear in the 19-21m/s wind speed bin is equal to 0.27 which is significantly more than the API value.

The land-based LiDAR average shear exponent of 0.20 exceeds the offshore DNV range of 0.08 to 0.13, the ABS values of 0.11 to 0.14, the previous study by Viselli et al and the Mesoscale model prediction. This data matches the 0.2 value recommended by IEC 61400-3 and exceeds the 0.16 value proposed by ASCE-7. As compared to API, the measured wind shear in the 19-21m/s wind speed bin is equal to 0.28 which is significantly more than the API value.

Differences in these comparisons could be due to lack of multiple complete years of data as well as site specific conditions not specifically addressed by the standards and past studies. Differences in winds shear has been observed to be diurnal and seasonal, as shown in Table 8 due to "the stability of the atmosphere which is governed by vertical temperature distribution from radiative heating or cooling of the earth's surface and the subsequent convective mixing of the air adjacent to the surface" [25]. This is especially true for offshore environments where there is a difference in sea and air temperature which affects the lower boundary layer. Thus wind speeds and therefore wind profiles are effected. Previous findings have shown that the stratification of the lower boundary layer is mainly unstable in the fall while stable in the spring [26].

The DeepCLiDAR was deployed for approximately 8 months from February to the end of October. Considering the mesoscale model outputs, averaging this partial year data set would tend to result in higher average wind shear considering that the majority of the winter months were not included in the average. This could explain the differences with the DNV, ABS, prior study, and the mesoscale model but would likely widen the gap against the IEC 61400-3 standard. The land-based LiDAR was deployed considerably longer for 21 months. However, the result of this additional data record is an increase in wind shear as compared to the offshore LiDAR which is not expected based on the mesoscale model which would expect a lower average wind shear to occur when more of the data from the winter months is considered. When considering specific data points considerably more deviation from the standards exists. The spread on the data for wind shear is highly variable and the values can increase or decrease significantly from the reported averages. In some cases, a negative wind shear occurs which is not well discussed in current offshore standards. This data set includes a number of negative wind shear values.

A comparison of the measured turbulence intensity against IEC standards is now presented. Figure 8, Figure 9, and Figure 10 present the measured turbulence from the land-based LiDAR and DeepCLiDAR. In addition to the measured data, the 90% percentile/ quantile of the measurements is provided for comparison against the IEC 61400-1 industry turbulence class turbulence intensity curves for Class A and Class C site conditions. The Land-based and DeepCLiDAR 90% quantiles fall below the class C curve for all wind speed bins above about 2m/s.

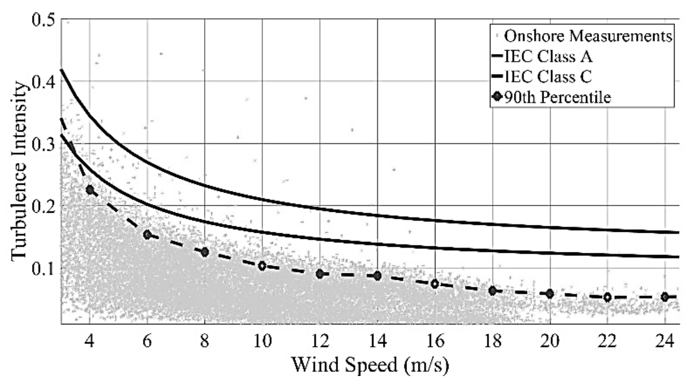


**Figure 8 Measured Land-Based Wind Turbulence Intensity v. 10-minute Mean Wind Speed at 100m**

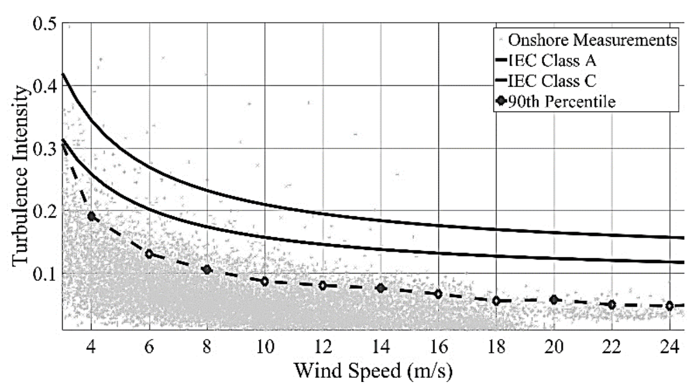


**Figure 9 Measured Land-Based Wind Turbulence Intensity v. 10-minute Mean Wind Speed at 100m Using Concurrent Data**

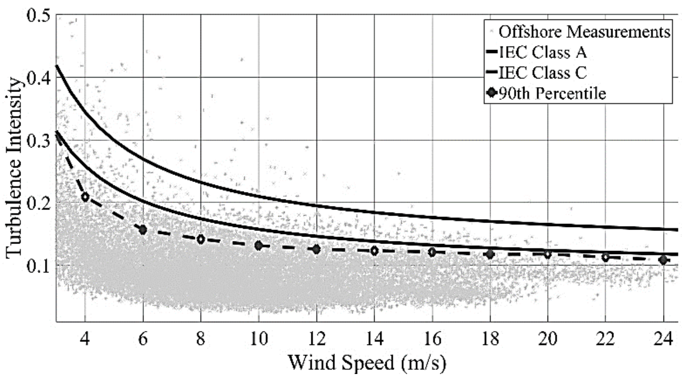


**Figure 10 Measured Offshore Wind Turbulence Intensity v. 10-minute Mean Wind Speed at 100m**

## SUMMARY AND CONCLUSIONS

A unique high altitude (40-200m) wind speed data set has been presented. The data was collected in the Northeast US in support of the development of the first floating offshore wind farm in the US planned for grid-connection by 2021. There is currently a lack of wind speed data at high altitudes in the US making these first measurements useful for understanding the wind conditions offshore in the US for future research and wind developments. This testing campaign consisted of two LiDAR wind measurement devices collecting data simultaneously. One was positioned on land and other offshore on a DeepCLiDAR buoy.

The data from this campaign suggests that wind shear varies throughout the year, with wind speed, and for different wave conditions. The mean measured wind shears exceeded those presented in most industry recommendations. It was not uncommon to see a wind shear coefficient above 0.20 with wind speeds above 10m/s. Industry standards generally present only a few wind shear values for all load cases. In reality wind shear varies significantly. Higher wind shear could have significant effect on the fatigue life for a wind turbine and support structure. For example, the loading on the blade will vary more with increased wind shear as it rotates.

Both onshore and offshore LiDAR wind turbulence measurements are not currently used as a reliable measurement. The data is presented in this paper because there is little offshore turbulence measurements available in the US. The data shows that the offshore wind turbulence at 100m was below IEC 61400-1 Class C.

In summary, this data campaign and analysis suggest that wind shear may need to be considered carefully given the significant variation possible and the higher than most industry standard mean value. Additional long term offshore wind data collection campaigns would help to confirm these findings.

## ACKNOWLEDGMENTS

The authors would like to acknowledge the support of the US Department of Energy Office of Energy Efficiency and Renewable Energy Grant Number DE-EE0002981 and DE-EE0003278, the State of Maine 2010 State Bond, the Maine Technology Institute grant number DL-4006, the Rockerfeller Brothers, the Davis Family Foundation, the University of Maine, the University of Maine Physical Oceanography Group, NRG Renewables, and AWS Truepower- UL.

## REFERENCES


[1] A. Viselli, H. Dagher, A. Goupee and C. Allen, "Design and Model Confirmation of the Intermediate Scale VolturnUS Floating Wind Turbine Subjected to its Extreme Design Conditions," *Wind Energy Journal,* vol. 19, no. 6, 2015.

[2] R. Newman, "Optimizing Lidar Wind Measurements from the DOE WindSentinel Buoys," Pacific Northwest National Laboratory, Richland, WA, 2016.

[3] M. Schwartz, D. Heimiller, S. Haymes and W. Musial, "Assessment of Offshore Wind Energy Resourses for the United States," Golden, CO, 2010.

[4] AWS Truewind, LLC, "New York's Offshore Wind Energy Development Potential in the Great Lakes: Feasibility Study," Albany, NY, 2010.

[5] A. Viselli, G. Forristall, B. Pearce and H. Dagher, "Estimation of Extreme Wave and Wind Design Paremeters for Offshore Wind Turbines in the Gulf of Maine Using a POT Method," *Ocean Engineering,* vol. 104, pp. 649-658, 2015.

[6] Y. L. Pichugina, R. M. Banta, W. A. S. S. P. Brewer and H. Michael, "Doppler Lidar-Based Wind-Profile Measurement System for Offshore Wind-Energy and Other Marine Boundary Layer Applications," *Journal of Applied Meteorology and Climatology,* vol. 51, no. 2, pp. 327-349, 15 February 2012.

[7] B. Lange, S. Larsen, J. Højstrup and B. R.J., "Importance of Thermal Effects and Sea Surface Roughness for Wind Resource and Wind Shear at Offshore Sites," *Wind Engineering and Industrial Aerodynamics,* vol. 92, no. 9, pp. 959-988, 2004.

[8] A. Pena Diaz, S.-E. Gryning, T. K. Mikkelsen, C. B. Hasager and M. C. Kelly, "The Modeling and Observation of the Long-Term Vertical Wind Profile and Wind Shear," in *In Proceedings of EWEA 2012 - European Wind Energy Conference & Exhibition European Wind Energy Association (EWEA),* Copenhagen Denmark, 2012.

[9] A. Pena Diaz, T. K. Mikkelsen, S.-E. Gryning, C. B. Hasager, A. N. Hahmann, M. Badger, I. Karagali and M. Courtney, "Offshore Vertical Wind Shear: Final Report on NORSEWInD's Work Task 3.1," DTU Wind Energy, Kongens Lyngby, Denmark, 2012.

[10] I. S. Øistad, "Analysis of the Turbulence Intensity at Skipheia Measurement Station," Norwegian University of Science and Technology, Trondheim, Norway, 2015.

[11] P. Argyle, S. Watson, C. Montavon, I. Jones and M. Smith, "Turbulence Intensity Withing Large Offshore Wind

Farms," in *European Wind Energy Association*, Paris, France, 2015.

[12] ABS, "Guide for Building and Classing Floating Offshore Wind Turbine Installations," American Bureau of Shipping, Houston, TX, 2013.

[13] IEC, *International Standard IEC 61400-03*, 1 ed., Geneva: International Electrotechnical Commission, 2009.

[14] DNV, "Environmental Conditions and Environmental Loads," Det Norske Vertias, Oslo, Norway, 2010.

[15] ASCE, "Minimum Design Loads for Buildings and Other Structures," American Society of Civil Engineers, USA, 2010.

[16] IEC, *International Standard IEC 61400-1*, Geneva: International Electrotechnical Commission, 2005.

[17] Carbon Trust, *Carbon Trust Offshore Wind Accelerator roadmap for the commercial acceptance of floating LiDAR technology,* CTC819 Version 1.0 ed., 2013.

[18] A. Viselli, M. Fillipelli, N. Pettigrew and D. HJ, "Validation of a LiDAR Wind Resource Assessment Buoy System in US Northeast Waters Against a Fixed Land-based LiDAR System," *Wind Energy Journal,* 2018 (Under Review).

[19] N. Pettigre, H. Xue, J. Irish, W. Perrie, C. Roesler, A. Thomas and D. Townsend, "The Gulf of Maine Ocean Observing System: Generic Lessons Learned in the First Seven Years of Operation (2001-2008)," *MTS Journal,* vol. 43, no. 3, pp. 91-102, 2008.

[20] H. A. Panofsky and J. A. Dutton, in *Atmospheric Turbulence: Models and Methods for Engineering Applications*, Wiley, 1984, p. 397.

[21] A. Sathe, J. Mann, N. Vasiljevic and G. Lea, "A Six-Beam Meathod to Measure Turbulence Statistics Using Ground-Based Wind LiDARS," *Atmospheric Measurment Techniques,* vol. 8, no. 2, pp. 729-740, 12 February 2015.

[22] A. Sathe, J. Mann, J. Gottschall and M. Courtney, "Can Wind Lidars Measure Turbulence?," *Journal of Atmospheric and Ocean Technology,* vol. 28, no. 7, pp. 853-868, 2011.

[23] J. F. Newman, T. A. Bonin, P. M. Klein, S. Wharton and R. K. Newsom, "Testing and Validation of Multi-LiDAR Scanning Strategies for Wind Energy Applications," *Wind Energy Journal,* vol. 19, no. 12, pp. 2239-2254, 16 March 2016.

[24] American Petroleum Institute, *Derivation of Metocean Design and Operating Conditions,* Washingon, DC: API Publishing Services, 2014.

[25] W. Frost and C. Aspliden, "Characteristics of Wind," in *Wind Turbine Technology Fundamental Concepts of Wind Turbine Engineering*, New York, ASME, 2009, pp. 488-492.

[26] J. Van Wijk, A. Belijaars and A. T. W. Holtslag, "Evalution of Stability Corrections in Wind Speed Profiles Over the North Sea," *Journal of Wind Engineering and Industrial Areodynamics,* vol. 33, no. 3, pp. 551-566, 1990.

[27] A. Truepower, "Buoy Based LiDAR Pre-Deployment Validation; DeepCLiDAR Validation-Phase III," 21 October 2016.